JOURNAL OF CATALYSIS 133, 342–357 (1992)

Comparison of Pt/KL Catalysts Prepared by Ion Exchange or Incipient Wetness Impregnation

D. J. OSTGARD,[1] L. KUSTOV,[2] K. R. POEPPELMEIER, AND W. M. H. SACHTLER*

V. N. Ipatieff Laboratory, Center for Catalysis and Surface Science, Northwestern University, Evanston, Illinois 60208

Received July 1, 1991; revised August 22, 1991

Pt/KL catalysts prepared by ion exchange (IE), incipient wetness impregnation (IWI), and coimpregnation with KCl (IWI + KCl) have been characterized by dynamic techniques, chemisorption of H_2 and CO, Fourier transform-infrared spectroscopy (FT-IR) of adsorbed CO, and catalytic tests using *n*-hexane (*n*-C6) and methylcyclopentane (MCP) conversions as probe reactions. Temperature-programmed reduction (TPR) shows significant differences between the IE and IWI catalysts. After calcination up to 400°C, the IWI samples contain Pt^{4+} ions that are reduced at 250°C, but IE samples contain PtO particles that are reduced at 11°C, besides two Pt^{2+} species with TPR peaks at 80 and 150°C. High-resolution electron microscopy, adsorption, FT-IR, and catalytic results consistently show that, after reduction, the IWI catalysts contain smaller Pt particles located inside the zeolite channels, while the IE sample has larger particles, some of which are on the external surface. At high temperature, excess KCl reacts with zeolite protons, forming HCl which escapes. In comparison to the IE samples, the IWI catalysts are less acidic, less active for *n*-C_6 conversion, more selective for dehydrocyclization, but less selective for hydrogenolysis, and they deactivate less. Since hydrogenolysis requires large Pt ensembles, the small Pt particles in the IWI catalysts produce less C_1–C_5 compounds and less coke. The product distribution of MCP ring opening shows higher than statistical selectivity toward 3-methylpentane, suggesting that the MCP molecule becomes oriented inside the zeolite channels.

1. INTRODUCTION

Since Bernard reported that Pt/KL is very selective for *n*-hexane aromatization (*1*), much research has been performed on this catalyst system. Some researchers use catalysts prepared by ion exchange (IE) (*2–4*), others prefer incipient wetness impregnation (IWI) (*5, 6*), while others use coimpregnation of KCl (IWI+KCL) (*7*). A systematic comparison of samples prepared by these methods appears desirable. In most procedures an aqueous solution of $Pt(NH_3)_4Cl_2$ is used for the addition of Pt to the zeolite. In the IE preparation $Pt(NH_3)_4^{2+}$ ions are exchanged against K^+ ions,

$$Pt(NH_3)_4^{2+} + 2Cl^- + 2K^+_{zeol} \rightarrow 2K^+_{(aq)} + 2Cl^-_{(aq)} + [Pt(NH_3)_4]^{2+}_{zeol}, \quad (1)$$

and the K^+ and Cl^- ions are removed by filtration and subsequent washes, while in the IWI technique these ions remain in the zeolite. After destruction of the NH_3 ligands, in the calcination step, Pt^{2+} ions coordinated to zeolite walls should be produced in the IE procedure, but some yet unknown distribution of Pt^{2+} ions and $PtCl_2$ particles, located in zeolite channels, will result after drying in the IWI preparation. This situation is further complicated by the fact that some reduction of Pt^{2+} ions or $PtCl_2$

[1] Present address: Degussa Corporation, Catalysts Division 104 New Era Drive, South Plainfield, NJ 07080.

[2] On leave from N. D. Zelinsky Institute of Organic Chemistry, Academy of Sciences, Moscow, Russia.

0021-9517/92 $3.00

particles by the action of decomposing NH_3 ligands is difficult to avoid. As a result of this "autoreduction" Pt particles will be formed which are oxidized to PtO and PtO_2 during further calcination. The relative concentrations of the various Pt species—ions, metal, chloride and oxide particles—will be strongly dependent on the preparation technique. No systematic study seems to be known in the open literature of the actual composition of the Pt species populating the zeolite channels prior to reduction. The present work tries to get some information on this matter by analyzing temperature-programmed reduction (TPR) profiles of Pt/KL catalysts after calcination.

The calcination step is followed by reduction with H_2. In this process protons of considerable Brønsted acidity will be formed from Pt^{2+} ions,

$$Pt^{2+} + H_2 \rightarrow Pt^0 + 2H^+, \qquad (2)$$

whereas HCl or H_2O is a co-product of reduction of $PtCl_2$ or Pt oxides, respectively. For the use of the monofunctional Pt/KL catalyst, acidity is highly undesirable; protons are known to lower selectivity to aromatics and catalyst stability (*1, 3*). Therefore the IWI procedure is usually preferred; even in this case it has been recommended that special precautions be taken to neutralize protons. This led to the addition of KCl to the impregnation solution, the rationale being that surface protons will react at elevated temperature with KCl according to the reaction:

$$H^+_{zeol} + KCl \rightarrow K^+_{zeol} + HCl. \qquad (3)$$

The HCl can then be driven off at the temperature of reduction (350°C).

Temperature-programmed techniques have been used successfully to characterize Pt (*8, 9, 11, 12*) and Pd (*10*) particles supported in Y zeolites. These techniques will be used in this research along with reaction studies, Fourier transform-infrared spectroscopy (FT-IR), and high-resolution electron microscopy (HREM) to characterize Pt particles incorporated into the KL zeolite. An important goal in the preparation of Pt/KL catalysts, besides neutralizing acid sites, is to obtain small Pt particles located inside the zeolite channels without blocking them. As calcination, reduction, and catalytic reaction require high temperatures, the ultimate Pt particle size and location are controlled mainly by the mobility of precursors and primary particles through zeolite channels. Electron microscopy has been used to identify the size and the location of the Pt particles in the reduced catalyst. The presence of large Pt particles will be related to the selectivity for metal cracking, which is generally assumed to require large Pt ensembles.

EXPERIMENTAL

2.1. Catalyst Preparation and Imaging

The 0.5% Pt/KL IE catalyst was prepared from KL zeolite purchased from Tosoh, Lot HSZ-500 KOA, by first stirring a suspension of 30 g of this zeolite in 3 liters of distilled water for 2 h, then adding dropwise 300 ml of distilled water containing 0.2715 g of $Pt(NH_3)_4Cl_2$ to the slurry over 8 h. After stirring for an additional 24 h, the slurry was filtered and washed with an aqueous NaOH solution of pH 10, until no Cl^- was detected in the fresh filtrate. The material was then dried in the Büchner funnel by drawing air through it for 24 h. The subsequent calcination was carried out in flowing ultrahigh-purity (UHP) O_2 at a flow rate of 1000 ml/min/g of catalyst, while the temperature was ramped from 25 to 400°C at a rate of 0.5°C/min and held at 400°C for 2 h. After purging in Ar at 400°C for 1 h, the sample was cooled to room temperature and stored in a desiccator containing a saturated aqueous NaCl solution. The 1.2% Pt/KL IE catalyst was made by the same method, except that 0.6515 g of $Pt(NH_3)_4Cl_2$ was used in the exchange procedure.

The 0.5% Pt/KL IWI catalyst was prepared by spraying 10 g of the KL zeolite with 5.7 ml of water containing 0.0911 g of $Pt(NH_3)Cl_2$. During the spraying procedure the round-bottom flask containing the zeolite was rotated. After impregnation, the sample was dried at 100°C for 24 h in a roto-

evaporator. The catalyst was then calcined and stored as described above for the IE catalyst. The 0.5% Pt/KL IWI + KCl catalyst was made by the same procedure as described for the IWI catalyst, with the exception that the impregnating solution contained 2 Pt equivalents of KCl. For preparation of the 1.2% Pt/KL IWI + KCl catalyst 0.6515 g of $Pt(NH_3)Cl_2$ was used in an otherwise identical procedure.

To investigate Pt distribution and dispersion in zeolite microcrystals transmission electron microscopic studies were carried out. Pt/KL samples prepared by IE and IWI + KCl methods were used after their reduction at 350°C in flowing H_2.

2.2. H_2 and CO Chemisorption

Volumetric chemisorption measurements were carried out at 25°C in a vacuum system with a Setra pressure detector. Usually 0.5 g of sample was used; it was dried in flowing UHP O_2 at a flow rate of 1000 ml/min/g with the temperature being ramped at a rate of 0.5°C/min from 25 to 400°C with a hold at 400°C for 2 h. The catalyst was then purged in UHP Ar at 400°C for 1 h, followed by cooling to 350°C. Reduction was carried out at 350°C for 2 h in UHP H_2, followed by evacuation to 5×10^{-6} Torr at 350°C for 1 h. The catalyst was cooled to 25°C while under vacuum before the adsorptive (H_2 or CO) was admitted in increments up to pressures of 70 Torr.

2.3. Temperature-Programmed Reduction and Temperature-Programmed Desorption

The apparatus and procedure for the temperature-programmed reduction (TPR) and desorption (TPD) experiments were described in previous papers (*8, 11*). Prior to TPR experiments the catalyst was dried in UHP O_2 at a rate of 1000 ml/min/g of catalyst with the temperature being ramped from 25 to 400°C at a rate of 0.5°C/min followed by a hold at 400°C for 2 h. The sample was cooled to 25°C in O_2 followed by purging in Ar for 30 min and cooling to −80°C in Ar. The gas was then switched to a 5% H_2/Ar mixture flowing at a rate of 25 ml/min. During the TPR experiment the temperature was ramped from −80 to 350°C at a rate of 8°C/min and the H_2 consumed was monitored by a TCD cell. The TPR experiment was then followed by a TPD run. Before TPD the catalyst was cooled from 350 to 25°C in the 5% H_2/Ar stream followed by a purge in Ar flowing at a rate of 25 ml/min for 20 min and cooling in Ar to −80°C. For subsequent TPD the temperature was ramped at a rate of 8°C/min up to 350°C, while H_2 evolution was monitored by a TCD detector. TPD experiments were also done for H_2 preadsorbed at 24°C for comparison to chemisorption experiments. In these TPD experiments the H_2 preadsorbed at 350°C, following the TPR, was purged off with Ar at 350°C for 1 h followed by cooling in Ar to 25°C. H_2 was then introduced to the catalyst for 30 min followed by a purge in Ar for 30 min before the TPD was performed in the same manner as described above. A second TPR run after the TPD experiments verified that no reoxidation of the Pt^0 by surface protons occurred during the TPD run. TPR experiments were also carried out after the catalyst was reoxidized at various temperatures. In these experiments the adsorbed H_2 from the previous TPR was purged off with Ar at 350° for 30 min followed by a change in the temperature to the desired reoxidation temperature in Ar. The catalyst was then reoxidized in O_2 for 1 h and the TPR was carried out as described above.

Blank runs with metal-free KL showed peaks at low temperature due to Ar desorption from the support; this was corrected for when quantitative TPR or TPD results were calculated from peak integration.

2.4. TPR-MS and Temperature-Programmed Reoxidation-MS

TPR-MS measurements were carried out in the same manner as described above ex-

cept that H_2 consumption, H_2O evolution, and HCl evolution were monitored by mass spectrometry. The gas downstream from the reactor is split, so that about one-half of the gas is vented; the remainder passes into a two-stage pressure reduction system. This consists of a capillary tube which is pumped down by a mechanical pump. The mass spectrometer continuously samples the gas mixture from the capillary tubing through a variable leak valve. It is pumped with a turbomolecular pump and operates at about 10^{-6} Torr. The mass spectrometer and the temperature programmer are interfaced to a personal computer for data acquisition. After TPR-MS the catalyst was purged with Ar at 350°C for 1 h, followed by cooling to −80°C at which the gas was switched to a 5% O_2/He mixture flowing at 40 ml/min. Temperature-programmed reoxidation was then carried out by ramping the temperature from −80 to 500°C at a rate of 8°C/min. O_2 consumption and the evolution of H_2 and H_2O were monitored by mass spectrometry. After TP reoxidation-MS runs, TPR-MS experiments were carried out on the same samples. For monitoring the evolution of HCl, the same temperature regimes and gas flow rates were used. However, pure hydrogen was used instead of H_2/Ar to avoid interference of HCl with the Ar isotopes ^{36}Ar and ^{38}Ar. For the same reason, samples were purged with He rather than Ar after calcination. As our mass spectrometer is less sensitive than our TCD cell, the MS experiments were carried out on 1.2% Pt/KL samples (IE and IWI + KCl).

2.5. *Catalytic Tests*

Methylcyclopentane (MCP) and *n*-hexane reactions were carried out at atmospheric pressure in a continuous-flow microreactor as described before (*14*). The experimental conditions were as follows: 350°C, a space velocity of 2000 ml/min/g of catalyst, and a H_2/hydrocarbon ratio of 20/1. The total conversion was always below 20% and the products were analyzed by an on-line gas chromatograph equipped with a FID detector. The pretreatment of these catalysts before the reaction was the same as for the chemisorption experiments except that no evacuation took place prior to the reaction.

2.6. *Temperature-Programmed Oxidation*

Temperature-programmed oxidation (TPO) experiments were conducted in a similar manner as described before (*15*). After 10-h catalytic tests with *n*-hexane, as described above, the catalyst was cooled to room temperature under flowing Ar. The microreactor was then sealed with Teflon valves and transferred to a manifold connected to a mass spectrometer as described above. Moisture in the dead volume of the microreactor was removed by three evacuation and Ar purge sequences before opening the valves isolating the catalyst. The catalyst was then cooled to −80°C in flowing Ar before the gas was switched to a 5% O_2/He mixture flowing at 40 ml/min. The temperature was ramped from −80 to 550°C at a rate of 8°C/min. During the TPO runs the consumption of O_2 and evolution of CO, CO_2, and H_2O were continuously monitored by mass spectrometry.

2.7. *Fourier Transform-Infrared Spectroscopy*

Thin self-supported wafers of the sample (without binders) with a thickness of approximately 7–13 mg/cm^2 and a diameter of 8 mm were pressed and placed into the sample holder of the IR cell described in (*16*). The spectra were measured at 27°C using a Nicolet 60SX Fourier transform spectrometer with a resolution of 1 cm^{-1}. Before the spectroscopic measurements the samples were heated in a 120 ml/min flow of O_2 from 27 to 497°C, ramping the temperature at 0.5°C/min, then holding at 497°C for 2 h. After calcination the system was purged with He at 497°C for 20 min before cooling the samples to 27°C in He. The reduction temperature was ramped from 27 to 347°C at a rate of 8°C/min and kept at 347°C for 20 min. Then the samples were purged at 347°

TABLE 1

H_2 and CO Chemisorption of 0.5% Pt/KL Catalysts

Preparation method	H_{ads}/Pt	CO_{ads}/Pt
Ion exchange (IE)	1.11	0.45
Incipient wetness impregnation (IWI)	0.95	0.69
IWI + KCl	1.01	0.51

with He for 20 min and cooled in flowing He to 27°C, and the background spectra of the reduced samples were measured. A 5/30 CO/He mixture was passed through the cell for 10 min at a flow rate of 70–80 ml/min and the cell was purged with He to remove gaseous CO.

RESULTS AND DISCUSSION

3.1. Chemisorption and Temperature-Programmed Desorption

The static chemisorption data expressed as H/Pt and CO/Pt ratios are compiled in Table 1 for the 0.5% Pt/KL catalyst. They agree well with values reported by Larsen and Haller (*3*). For the IE preparation the H/Pt ratio calculated from TPD in Table 2 is in good agreement with the value determined by static chemisorption. However, for the IWI catalysts (with and without KCl) integration of the TPD profiles, obtained after adsorption of H_2 at 350°C, results in higher H/Pt values than found by chemisorption of H_2 at room temperature. As seen in Tables 1 and 2, both methods consistently give the same value, within experimental error, for the IWI and IWI + KCl 0.5% Pt/KL samples. To verify whether the difference in adsorption temperature is responsible for the different H/Pt values, we also measured TPD after adsorption at 24°C. These data are given in the second column of Table 2; they are in perfect agreement with the data in Table 1. It follows that for the samples prepared by impregnation, the amount of hydrogen chemisorbed at 24°C is about one-half that chemisorbed at 350°C followed by cooling in H_2.

The CO/Pt ratio is smaller than the H/Pt value for all samples. The high H/Pt ratios indicate that in all catalysts studied in this work the Pt particles are very small. Evidently, not all Pt atoms that are accessible to H_2 are also accessible to the larger CO molecule. Some channel blocking by Pt particles appears conceivable. It follows that some Pt atoms may also be inaccessible to the probe reactants used here; therefore, we decided to base the turnover frequencies (TOFs) for the catalytic results on the CO/Pt ratios (*17*). It is noteworthy that a lower CO/Pt ratio is found for the 0.5% Pt/KL IWI + KCL catalyst than for the 0.5% Pt/KL IWI catalyst. This finding suggests some channel blocking by some combination of excess KCl and Pt clusters inside the zeolite channels.

3.2. Temperature-Programmed Reduction

Figure 1 shows the initial TPR of the 0.5% Pt/KL IE catalyst and the effect of different reoxidation temperatures on the TPR profile. Integration of these profiles gives the total hydrogen consumptions, shown in Table 3. It is clear that the Pt valence in the catalysts prepared by the IE method is about 2+ in all cases. Small differences in the calculation of these valences may be due to uncertainties in the Ar desorption peak, as discussed earlier. In the initial TPR profile three peaks exist at 11, 80, and 150°C. Upon reoxidation at 25°C the second TPR spec-

TABLE 2

TPD Data for 0.5% Pt/KL Catalyst

Preparation method	H_{ads}/Pt, T_{ads} = 350°C	H_{ads}/Pt, T_{ads} = 24°C
Ion exchange (IE)	1.10	
Incipient wetness impregnation (IWI)	2.14	1.02
IWI + KCl	1.93	1.02

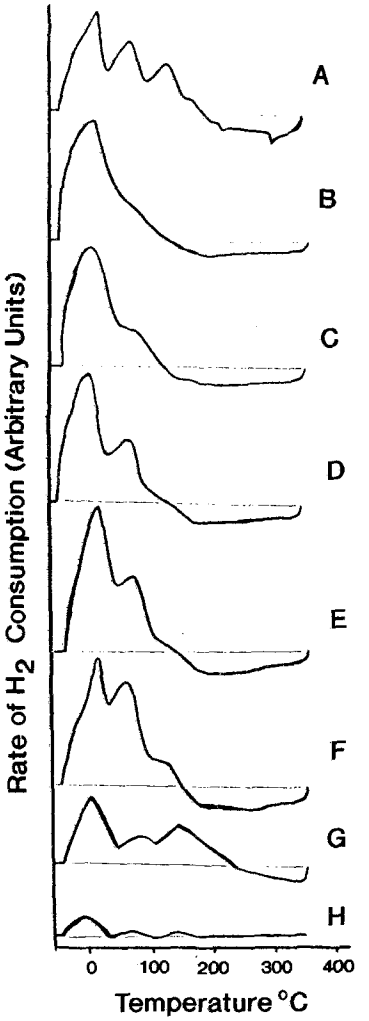

FIG. 1. Temperature-programmed reduction spectra for the 0.5% Pt/KL IE catalyst. (A) Calcined to 400°C. (B) reoxidized at 25°C. (C) reoxidized at 100°C. (D) reoxidized at 200°C. (E) reoxidized at 300°C. (F) reoxidized at 400°C. (G) reoxidized at 500°. (H) TPR Ar Desorption from the KL zeolite without Pt.

trum shows only the 11°C peak, while the 80°C peak emerges only if the reoxidation temperature is ≥ 200°C. The 150°C peak appears only if the reoxidation temperature is ≥ 500°. In general, the TPR profile shifts to higher temperatures with increasing reoxidation temperature. These data suggest that the chemistry of heating Pt/KL-IE in O_2 is similar to that identified previously for Pd/NaY-IE: at low temperature PtO is formed, which can be identified by its low temperature TPR peak; at higher temperature PtO reacts with zeolite protons to Pt^{2+} ions + H_2O.

Figure 2 shows the same sequence of TPRs for the 0.5% Pt/KL IWI+KCl cata-

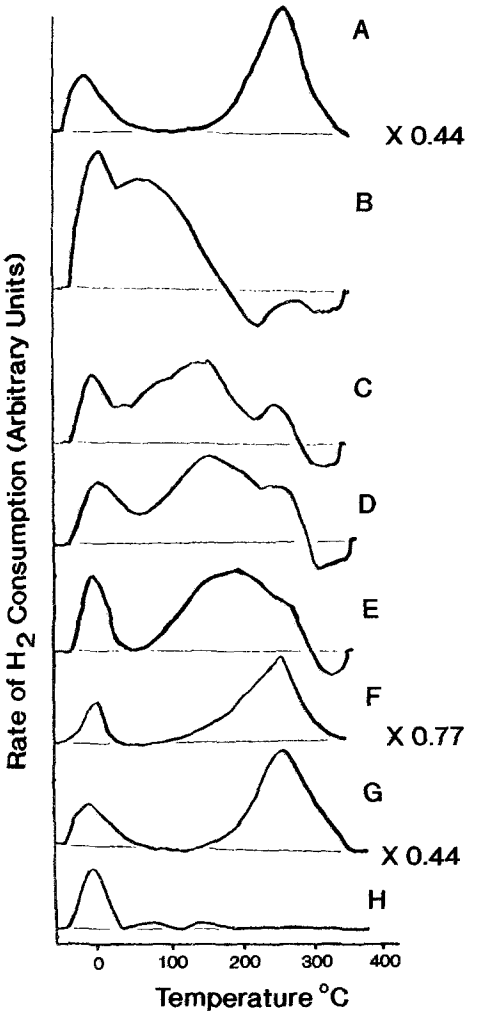

FIG. 2. Temperature-programmed reduction spectra for the 0.5% Pt/KL IWI + KCl catalyst. (A) calcined to 400°C. (B) Reoxidized at 25°C. (C) Reoxidized at 100°C. (D) Reoxidized at 200°C. (E) Reoxidized at 300°C. (F) Reoxidized at 400°C. (G) Reoxidized at 500°C. (H) TPR Ar desorption from the KL zeolite without Pt.

TABLE 3

TPR Data for the 0.5% Pt/KL Catalysts

Preparation method	Oxidizing treatment	Apparent Pt valence
IE	Calcined up to 400°C	1.99
IE	Reoxidized at 25°C	1.98
IE	Reoxidized at 100°C	2.04
IE	Reoxidized at 200°C	2.01
IE	Reoxidized at 300°C	2.28
IE	Reoxidized at 400°C	2.02
IE	Reoxidized at 500°C	2.08
IWI	Calcined up to 400°C	3.2
IWI	Reoxidized at 400°C	2.12
IWI + KCl	Calcined up to 400°C	4.00
IWI + KCl	Reoxidized at 25°C	1.94
IWI + KCl	Reoxidized at 100°C	2.09
IWI + KCl	Reoxidized at 200°C	2.11
IWI + KCl	Reoxidized at 300°C	1.98
IWI + KCl	Reoxidized at 400°C	2.16
IWI + KCl	Reoxidized at 500°C	3.68

lysts. The difference between these and the IE samples is striking. The initial TPR has a peak at 250°C; integration shows a Pt valence of 4+. The reduction peak at 250°C is assigned to the reduction of Pt^{4+} ions. Lieske *et al.* (*18*) found that Pt/Al_2O_3 catalysts prepared by impregnation of H_2PtCl_6 display Pt^{4+} ions after calcination; they are reduced at 250°C. In the present work the catalyst precursor is a Pt^{2+} salt; if autoreduction occurs under calcination conditions and the resulting Pt^0 atoms are oxidized, one would have to assume that PtO_2 is formed to account for a Pt valence of 4+. This oxide could subsequently react with surface protons to generate water and Pt ions.

Upon reoxidation between the temperatures of 25 to 400°C a different state of Pt is established; integration of the second TPR profile reveals a Pt valence of 2+. However, if reoxidation is carried out at 500°C, the following TPR profile shows that the valence of Pt is, again, 4+. This valence state was never observed for the IE samples. A common element, however, is that the TPR profile shifts to higher temperatures as the reoxidation temperature increases.

Whereas differences between IE and IWI + KCl preparations have been expected for the first TPR after initial calcination, it is surprising that the samples still "remember" their original preparation conditions after reduction and reoxidation. We assume that the presence of Cl^- ions is essential for this chemistry; i.e., the coordination and possibly also the location of the Pt ions will be different in the presence and absence of Cl^- (*18*).

The TPR results of the 0.5% Pt/KL IWI catalysts in Fig. 3 show some similarity to those of the 0.5% Pt/KL IWI + KCl samples. Again, the calculated valence of Pt exceeds 2+; it drops from 3.2+ to 2.12+. After reoxidation, the TPR profile shifts to lower temperatures. However, the initial TPR profile for this catalyst is less structured than that of the IWI + KCl catalyst. Reduction peaks at low temperature indicate that initially some Pt^{2+} ions or PtO particles are present, in accordance with the observed average valence lower than 4+.

To discriminate between Pt^{2+} ions and PtO particles, we used mass spectrometry, since only reduction of PtO or its reaction

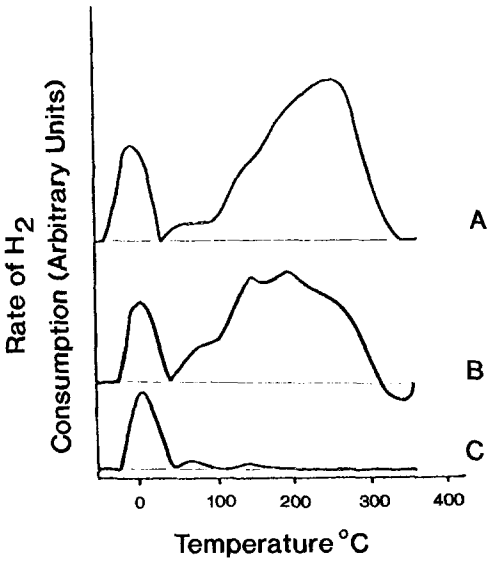

FIG. 3. Temperature-programmed reduction spectra for the 0.5% Pt/KL IWI catalyst. (A) Calcined to 400°C. (B) Reoxidized at 400°C. (C) TPR Ar desorption from the KL zeolite without Pt.

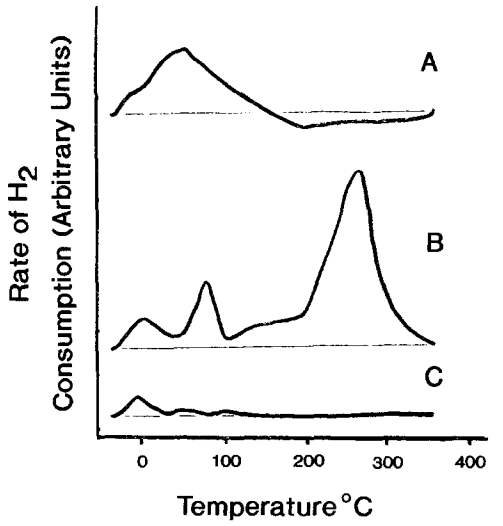

FIG. 4. Temperature-programmed reduction for the 1.2% Pt/KL Catalysts. (A) IE. (B) IW + KCl. (C) TPR Ar desorption from the KL zeolite without Pt.

with zeolite protons will produce water. A sequence of TPR-MS, followed by TP reoxidation-MS, and TPR-MS was used. Since mass spectrometry in our setup is less sensitive than the TCD, we prepared 1.2% Pt/KL analogs of the IE and IWI + KCl catalysts for these experiments. The TPR spectra, monitored by the TCD, are shown in Fig. 4 for these catalysts to facilitate comparison to the TPR-MS experiments. Surprisingly it appeared that the TPR profiles of these samples are also dependent on the metal loading. The TPR profiles shifted to lower temperatures with increasing metal loading. Figure 5 shows the TPR-MS, TP reoxidation-MS, and TPR-MS sequence for the 1.2% Pt/KL IE catalyst. The initial TPR-MS shows that water is the product of Pt reduction, indicating that the TPR peak at 11°C results from the reduction of PtO. PtO can be formed during calcination by oxidation of the Pt^0 generated via the autoreduction process shown in reaction (4). The water peak in this spectrum does not mirror that of H_2 consumption. The reason for this may be that the water is trapped in the zeolite and leaves it only at higher temperatures. The TP reoxidation-MS spectrum indicates that O_2 consumption occurs at 200°C; it is mirrored by H_2O evolution. This may be the result of PtO formation followed by the formation of Pt^{2+} via the reaction,

$$2(\text{-T-O-H}) + \text{PtO} \rightarrow \text{H}_2\text{O} + \text{Pt(O-T)}_2, \quad (4)$$

where T stands for Al and Si. The rate of this reaction also increases, as the reoxidation temperature is increased from 210 to 500°C, forming additional ions. The ion formation at 200°C during TP reoxidation-MS correlates well with the formation of the 80°C TPR peak in Fig. 3 as the reoxidation temperature surpasses 200°C. The formation of ions as the TP reoxidation approaches 500°C also correlates with the 150°C TPR peak after reoxidation at 500°C. The TPR-MS after reoxidation confirms the presence of Pt^{2+} in that a new reduction peak appears at 150°C and less water is formed.

In Fig. 6 the TPR-MS, TP reoxidation-MS, and TPR-MS spectra sequences of the 1.2% Pt/KL IWI + KCl catalyst are displayed. A slow evolution of HCl is observed in TPR-MS, starting at 80°C and rising until the temperature reaches 250°C. Upon further raising the temperature the HCl evolution rate remains constant. This HCl formation is attributed to reaction (3), which is the important mechanism to remove protons from the catalyst surface. It is interesting, that no well-defined HCl peak is observed in the TPR-MS profile, although one might expect that HCl formation becomes substantial near 250°C where Pt^{2+} ions are reduced and protons are formed by reaction (2). Apparently, proton formation is not the rate-limiting step for HCl evolution. The HCl formation below 250°C is indicative of a reaction with protons which were formed during autoreduction of Pt by decomposing ammine ligands.

The TP reoxidation-MS spectra show that O_2 consumption starts slowly at 10°C and peaks at 200°C. A second O_2 consumption peak occurs between 410 and 500°C. The valence of the Pt ions resulting from reoxidation at 25 to 400°C is only 2+. Reoxida-

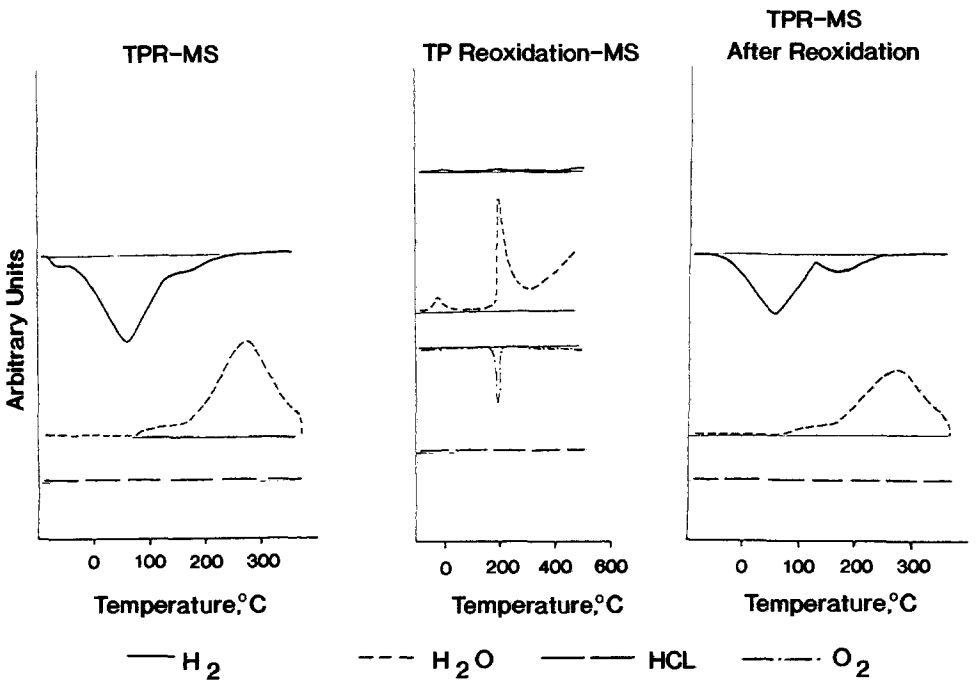

FIG. 5. TPR-MS, TP reoxidation-MS, and TPR-MS after reoxidation spectra for the 1.2% Pt/KL IE Catalyst.

tion at 500° results in the re-formation of Pt^{4+} ions. Surprisingly, a large amount of water is formed during reoxidation of this sample, indicating that it still contains a sufficient concentration of protons to convert Pt oxides into Pt ions and water by a reaction of type (4). This interpretation is confirmed by the MS data of the following reduction: only a small amount of water is detected, showing that reduction follows mainly reaction (2). The second TPR-MS spectrum, after reoxidation, is virtually identical with the initial TPR-MS spectrum, confirming that Pt^{4+} ions are regenerated. However, in view of the FT-IR data (see below) it appears that protons of very low Brønsted acidity are formed. The OH groups formed by this reduction are conceivably located in cancrinite cages, where they are inaccessible to gaseous molecules, and their interaction with Pt particles in the main channel will be weak.

Electron micrographs such as those shown in Fig. 7 and 8 show that more than 90% of the noble metal is dispersed within the zeolite channels, when prepared by IWI or IWI + KCl, in contrast to the IE catalyst, where large metal particles are observed on the exterior of the zeolite crystallites.

3.3. *n-Hexane Conversion*

Relevant data for *n*-hexane conversion at atmospheric pressure are listed in Tables 4–7 for the 0.5% Pt/KL catalysts. The IWI samples (with and without KCl) are less active than the IE sample, but they have higher benzene selectivities and lower C_1–C_5 selectivities, and show less deactivation with time on stream. There is not much difference between the IWI and the IWI + KCl as far as benzene selectivity is concerned, but the IWI + KCl catalyst deactivates more rapidly in spite of its lower C_1–C_5 selectivity. The cracking patterns of these catalysts indicate that C_1, C_2, C_4, and C_5 predominate for the IWI catalysts, whereas for the IE

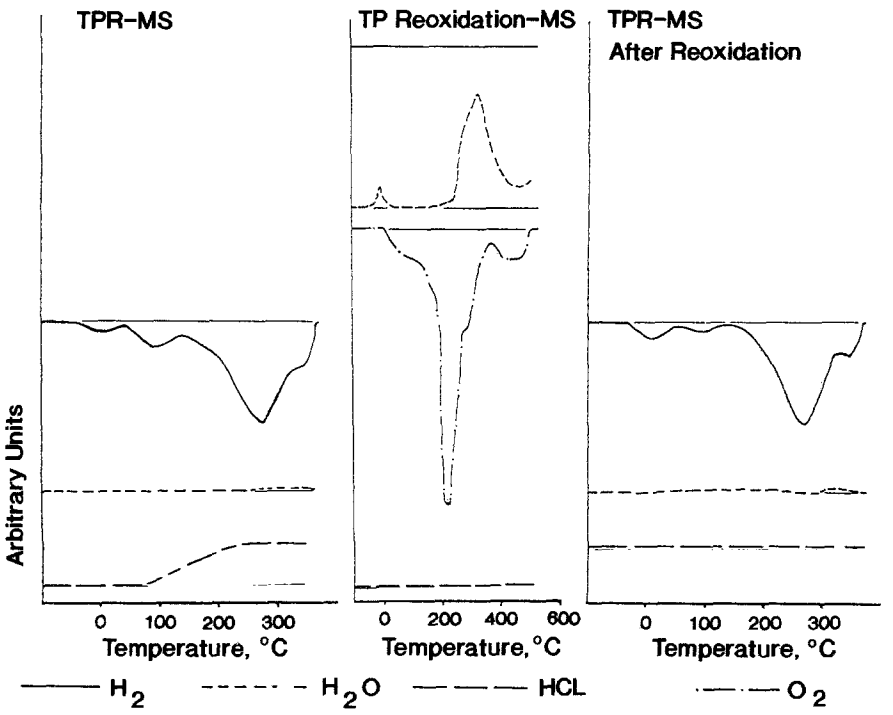

FIG. 6. TPR-MS, TP reoxidation, and TPR-MS after reoxidation spectra for the 1.2% Pt/KL IW + KCl catalysts.

sample C_3 is produced in relatively large amounts. The cracking patterns for the IWI catalysts indicate that the KL channel directs the *n*-hexane molecule to preferentially terminal carbon adsorption on the small Pt particles located inside the channel. As large Pt particles are known to catalyze internal fission of hydrocarbons, the large amount of C_3, in the cracking product of the IE catalyst, suggests that this hydrogenolysis will be catalyzed by large Pt particles at the external surface of the zeolite. If so, not all of the metal is located in the channels for this catalyst. This is confirmed by the FT-IR data (see below). The terminal cracking index (TCI = n-C_5/n-C_4) increases parallel to the benzene selectivity. These results are in agreement with those of Tauster and Steger (*4*), who proposed that an enhanced probability of terminal carbon adsorption is the cause for both a high terminal cracking index and a high benzene selectivity of *n*-hexane dehydrocyclization. The underlying concept of molecule orientation in the pores of the L zeolite is further supported by the product distribution of methylcyclopentane (see below).

After the end of a catalytic run, the carbonaceous deposits were analyzed by temperature-programmed oxidation. The TPO spectra are shown in Fig. 9; the chemical analysis of the coke, derived from the mass balance, is given in Table 8. The data show that the amount of coke formation follows the same trend as catalyst deactivation, as seen in Table 7. The TPO spectra consist of a peak at 200°C, ascribed to coke on the metal particles, and a shoulder peak at 280°C, assigned to coke deposited on nonmetal sites, which might be acidic.

3.4. Methylcyclopenteane Conversion

MCP reaction data for the 0.5% Pt/KL catalysts are listed in Tables 9–12. As the

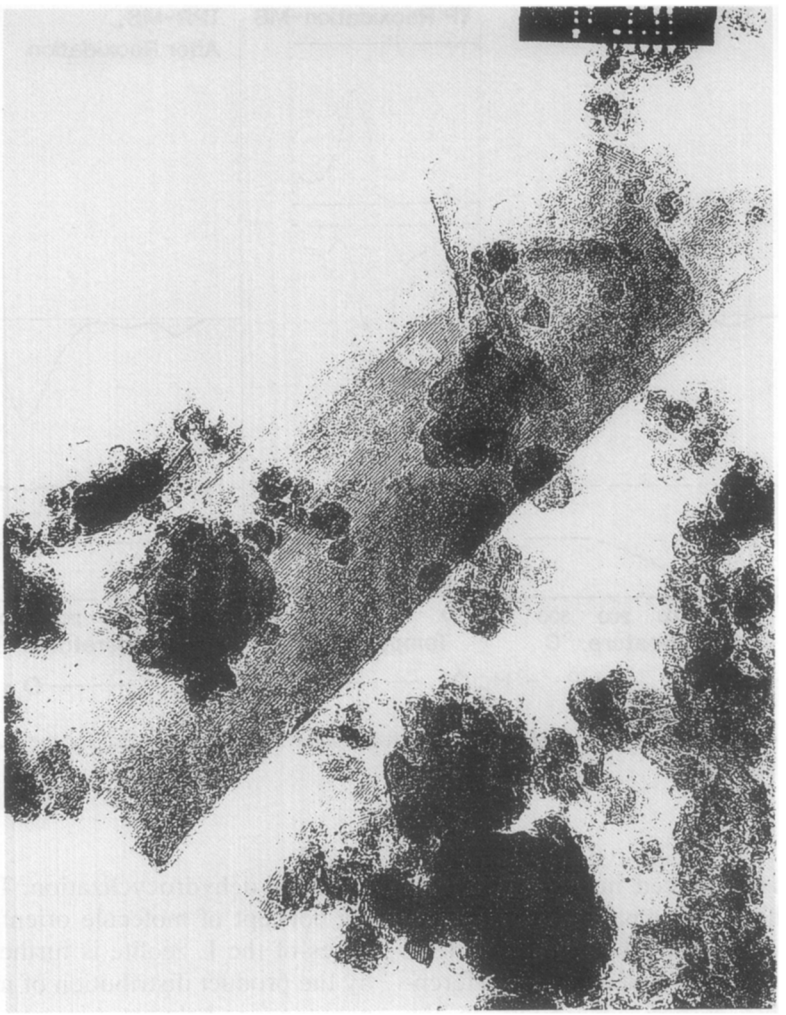

FIG. 7. Electron micrograph of Pt/KL IWI + KCl catalyst.

rate of MCP ring enlargement is known to be strongly enhanced by the presence of acid sites (*19*), the ring enlargement/ring opening (RE/RO) ratio has been used as a measure of catalyst acidity. Using this criterion, the IE catalyst appears to have a higher acidity than the other samples. Of the IWI catalysts, the KCl-free sample appears to be more acidic than the KCl coimpregnated one. This trend of acidity is in agreement with the other acid site-sensitive experiments reported in this paper (FT-IR and TPO). The results suggest that more acid sites are created by the reduction of Pt^{2+} ions in reaction (2) than by the reduction of an impregnated Pt salt, giving, e.g., HCl as the co-product of reduction. The results also suggest that reaction (3) is an efficient means of removing Brønsted sites from the catalysts.

The MCP conversion is capable of providing valuable information on the microgeometry surrounding active metal sites. Small Pt particles on an amorphous support were found by Gault to give a statistical distribution of ring opening products, i.e., 2-methylpentane:3-methylpentane:*n*-hexane = 2 : 1 : 2 (*20*). Table 12 shows that

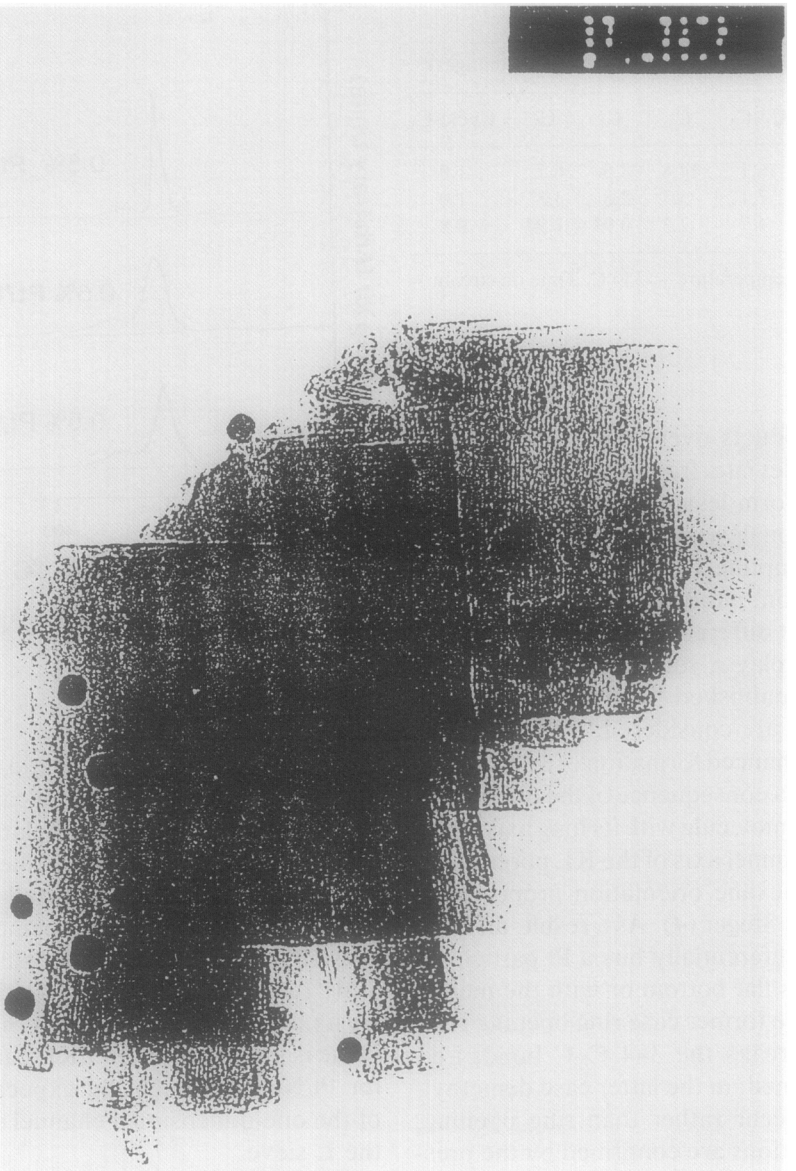

FIG. 8. Electron micrograph of Pt/KL IE catalyst.

TABLE 4

n-Hexane Turnover Frequencies (min^{-1}) for the 0.5% Pt/KL Catalysts[a]

Catalyst	C_1–C_5	2-MP	3-MP	MCP	Bz	Reaction
IE	2.10	0.60	0.35	0.77	0.68	4.50
IWI	0.61	0.40	0.28	0.72	1.01	3.02
IWI + KCl	0.29	0.37	0.29	0.84	0.91	2.70

[a] Reaction temperature = 350°C. Time on stream = 20 h.

TABLE 5

n-Hexane Mole Percentage Selectivities for the 0.5% Pt/KL Catalysts[a]

Catalyst	C_1–C_5	2-MP	3-MP	MCP	Bz
IE	46.7	13.3	7.8	17.1	15.0
IWI	20.2	13.2	9.3	23.8	33.4
IWI + KCl	10.7	13.7	10.7	31.1	33.7

[a] Reaction temperature = 350°C. Time on stream = 20 h.

TABLE 6

n-Hexane C_1–C_5 Selectivities (Mole Percentages)[a]

Catalyst	C_1–C_2	C_3	C_4	C_5	Cyclo-C_5
IE	16.1	14.8	8.0	6.7	1.0
IWI	7.1	5.7	2.8	3.5	1.0
IWI+KCl	4.7	2.3	0.93	1.94	0.8

[a] Reaction temperature = 350°C. Time on stream = 20 h.

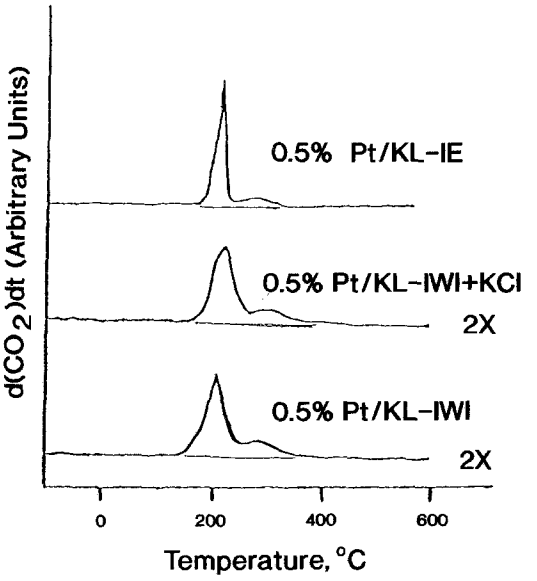

FIG. 9. TPO spectra for the 0.5% Pt/KL IE, IWI+KCl, and IWI catalysts.

the RO products over Pt/KL catalysts significantly deviate from the statistical pattern: they form less *n*-C_6, and more 3-MP. For the rationalization of this stereoselectivity it is tempting to consider a geometric interpretation, although it is not possible to exclude that different electronic states of Pt might also play a role. Geometric models have been published before (*21, 22*). Two phenomena are considered:

1. The enhanced formation of 3-MP is proposed to be a consequence of the orientation of the MCP molecule with its long axis parallel to the channel axis of the KL pores, similar to the hexane orientation proposed by Tauster and Steger (*4*). As a result, an MCP molecule preferentially hits a Pt particle either with its flat bottom or with the methyl group. In the former case ring opening preferentially breaks the 3–4 C–C bond, i.e., 3-MP is formed; in the latter case demethylation will occur rather than ring opening. Both predictions are confirmed by the present results: the 3-MP/2-MP ratio exceeds the statistical value of 0.5 significantly; in the cracking pattern the demethylation product cyclopentane is prominent. The former result has recently been reported by Alvarez and Resasco (*23*) in full agreement with the present data. A higher than statistical 3-MP/2-MP ratio was noted before for Pt/NaY catalysts, but the deviation from the statistical value is greater for the Pt/KL catalysts than for Pt/NaY, as might be expected in view of the one-dimensional channel structure of the L sieve.

2. For ring opening of MCP to yield *n*-C_6, it is probable that the MCP is initially chemi-

TABLE 7

n-Hexane Reaction Data[a]

Catalyst	TCI	2-MP/3-MP	% $\text{Deactivation}_{0.3\text{-}20\ h}$
IE	0.95	1.56	61.2
IWI	1.24	1.43	20.5
IWI+KCl	2.09	1.28	39.1

[a] Reaction temperature = 350°C. Time on stream = 20 h.

TABLE 8

TPO Data for the 0.5% Pt/KL Catalyst

Catalyst	C/Pt	C/H
IE	9.0	1.70
IW	4.1	1.60
IW+KCl	4.7	1.45

TABLE 9

MCP Turnover Frequencies (min^{-1}) for the 0.5% Pt/KL Catalysts[a]

Catalyst	C_1–C_5	MCP[2−]	2-MP	3-MP	n-C_6	Bz	Reaction
IE	0.53	0.60	1.50	0.92	1.0	1.51	6.06
IW	0.40	0.66	4.22	3.40	3.16	1.98	13.82
IW+KCl	0.25	0.62	2.46	1.94	1.89	1.64	8.8

[a] Reaction temperature = 350°C. Time on stream = 20 h.

TABLE 11

Selectivities for the 0.5% Pt/KL Catalysts[a]

Catalyst	C_1+C_2	C_3	C_4	C_5	Cyclo-C_5
IE	5.02	1.03	0.50	0.80	1.4
IWI	1.60	0.30	0.10	0.20	0.60
IWI+KCl	1.60	0.40	0.10	0.20	0.50

[a] Reaction temperature = 350°C. Time on stream = 20 h.

sorbed with its tertiary carbon atom, by breaking the C–H bond. Therefore only one face of the MCP molecule is active for this chemisorption. Since the zeolite channel impedes the MCP molecule from rolling over, only one-half of the molecules impinging with the tertiary C atom near a Pt site will be able to enter this reaction channel leading to n-C_6 formation. This restriction causes the n-C_6/2-MP ratio to be less than the statistical value of 1 : 1, in agreement with the observed results (*21*).

Both deviations of the experimental ratios from their statistical values and from the experimental data of Pt on amorphous catalysts are indicative for the fraction of Pt located inside the channels of the zeolite. The present data thus show that the IWI catalysts have a larger fraction of the Pt inside the channels than the IE sample. This is in agreement with the above conclusion based on the product pattern of n-hexane hydrogenolysis.

3.5. Fourier Transform-Infrared Data

FT-IR spectra of the Pt/KL IE, Pt/KL IWI, and Pt/KL IWI+KCl samples, all measured in the region of the stretching vibration of hydroxyl groups, were published in a recent paper (*24*); therefore they are not reproduced here. An intense band at 3740 cm^{-1} is ascribed to terminal silanols located at the external surface of zeolite; whereas bands at or near 3690 cm^{-1} are assigned to nonacidic hydroxyl groups. Bands in the region 3650–3630 cm^{-1} are assigned to acidic bridging hydroxyls. Both acidic and nonacidic hydroxyls are apparently produced during reduction of Pt ions. The bands are weak for all Pt/KL samples under study, but the intensity of the acidic bridging hydroxyl bands shows a clear trend; it decreases from IE via IWI to IWI+KCl.

Of special relevance are FT-IR spectra of CO adsorbed at room temperature on the same Pt/KL samples. These spectra have been published in the same paper (*24*). The predominant band on all samples is in the

TABLE 10

MCP Selectivities Mole Percentages for the 0.5% Pt/KL Catalysts[a]

Catalyst	C_1–C_5	MCP[2−]	2-MP	3-MP	n-C_6	Bz
IE	8.6	9.8	24.4	15.0	17.6	24.6
IWI	2.9	4.8	30.5	24.6	22.9	14.3
IWI+KCl	2.8	7.0	28.0	22.0	21.5	18.6

[a] Reaction temperature = 350°C. Time on stream = 20 h.

TABLE 12

MCP Reaction Data for the 0.5% Pt/KL Catalysts[a]

Catalyst	2MP/3MP	n-C_6/3MP	n-C_6/2MP	RE/RO
IE	1.63	1.18	0.72	0.43
IWI	1.24	0.93	0.75	0.18
IWI+KCl	1.27	0.97	0.77	0.26

[a] Reaction temperature = 350°C. Time on stream = 20 h.

range ν_{CO} = 2070–1950 cm^{-1}, with maxima at 2067, 2051, 2031, 2008, 1998, and 1979 cm^{-1}. These are due to linear CO on Pt, but show a remarkable dependence on the sample preparation. Bands which may be attributed to the bridging CO are very weak, and the band which is typical for CO adsorbed on large Pt particles (*25*) is totally absent. The total intensity of the bands attributed to Pt carbonyls (2067–1760 cm^{-1}) is significantly higher for Pt/KL-IWI than for Pt/KL-IE, showing that the metal dispersion is highest in Pt/KL-IWI, while the Pt/KL-IWI + KCl sample presents an intermediate case close to Pt/KL-IE. The band intensity data thus confirm the sequence for the Pt dispersion derived above from the direct CO chemisorption data.

The spectra show that various discrete states exist for the adsorbed CO; the relative abundances of these states depend greatly on the preparation conditions. For linear CO, the bands at 2067–2051 cm^{-1} predominate for the IE sample. In contrast, the band at 2031 cm^{-1} is the most intense for Pt/KL-IWI; also, the bands at 2008–1998 cm^{-1} are rather strong. For the zeolite coimpregnated with KCl the bands at 2008–1998 cm^{-1} are predominant; in addition, the intensity of the bands of bridging carbonyls is higher than for the other samples.

The results can be rationalized in terms of different electronic states of Pt. According to Besoukhanova *et al.* (*25*) and Larsen and Haller (*26*) a low frequency for linear Pt carbonyls is indicative of the low extent of "electron deficiency" of the Pt particles. As our previous data strongly suggest that "electron deficiency" is due to the formation of Pt–proton adducts, the frequency of the CO band should be shifted to higher values with increasing proton concentration. Indeed, the CO spectrum of the IE sample shows maximum intensity for the high-frequency band of the linear CO.

A result of the incipient wetness method is that counterions, e.g., Cl^-, must be present. They are instrumental in removing Brønsted protons, e.g., as HCl according to Eq. (3). This is confirmed by the absence of acidic hydroxyls for Pt/KL-IWI and Pt/KL-IWI + KCl. In the absence of protons the positive charge on the Pt particles is expected to be low, which is in agreement with the predominance of the low-frequency bands. An excess of KCl further decreases the concentration of residual protons and thus of the charge on the Pt particles. This is in accordance with the predominance of the low-frequency bands in the IR spectrum of adsorbed CO.

4. CONCLUSIONS

The following conclusions emerge from the experimental data presented in this paper:

1. Size and location of Pt particles and their precursors in zeolite KL depend strongly on the method of introducing the precursor, e.g., by ion exchange (IE), impregnation by incipient wetness (IWI), or coimpregnation of the Pt salt with KCl (IWI-KCl).

2. Catalysts prepared by IE contain, after calcination at 400°C, PtO particles that are reduced at 11°C and two forms of Pt^{2+} ions that are reduced at 80 and 150°C, respectively.

3. Catalysts prepared by IWI contain, after calcination, predominantly Pt^{4+} ions with a minority of Pt^{2+} ions. In the calcined IWI + KCl catalyst virtually all Pt is present as Pt^{4+} ions.

4. After reduction the Pt particles of the IWI catalysts (both with and without KCl) are located predominantly inside the channels, while in the IE sample part of the metal is located on the external zeolite surface.

5. The acidity of all Pt/KL catalysts is low. The order of increasing acidity is IWI + KCl < IWI < IE. This confirms that protons are formed in the reduction of Pt ions and that KCl reacts with protons to give HCl, which escapes. FT-IR of adsorbed CO indicates that in the IE samples some electron-deficient Pt–proton adducts might be formed.

6. A preferred C–C scission of methylcyclopentane (MCP) between C atoms 3 and 4 leads to a higher than statistical concentration of 3-methylpentane in the ring opening product. This can be rationalized by assuming that the MCP molecules are oriented inside the channels of KL with their long axis roughly parallel to the pore axis.

ACKNOWLEDGMENTS

We gratefully acknowledge support from the U.S. Department of Energy, Grant DE-FGO2-87ERA3654; from AKZO Corporate Research America; and from the NSF, Grant DMR-8915897. A Yu. Stakheev and S. Gandhi are thanked for their valuable contribution to the MS analysis of the HCl release. M. Treacy of Exxon Research and Engineering Company is thanked for providing the electron micrographs.

REFERENCES

1. Bernard, J. R., *in* "Proceedings, 5th International Conference on Zeolites, Heyden, London, 1980," p. 66.
2. Foger, K., and Jaeger, H., *Appl. Catal.* **56,** 137 (1988).
3. Larsen, G., and Haller, G. L., *Catal. Lett.* **3,** 103 (1989).
4. Tauster, S. J., and Steger, J. J., *J. Catal.* **125,** 387 (1990).
5. Hughes, T. R., Buss, W. C., Tamm, P. W., and Jacobson, R. L., "New Developments in Zeolite Science and Technology," pp. 725–732. Kodansha–Elsevier, Tokyo, 1986.
6. Lane, G. S., Modica, F. S., and Miller, J. T., *J. Catal.* **129,** 145 (1991).
7. Poeppelmeier, K., R., Trowbridge, T. D., and Kao, J., U.S. Patent 4,568,656.
8. Tzou, M. S., Teo, B. K., and Sachtler, W. M. H., *J. Catal.* **113,** 220 (1988).
9. Poeppelmeier, K. R., Funk, W. G., Steger, J. J., Fung, S. C., Cross, V. R., and Kao, J., U.S. Patents 4,595,668 and 4,648,690.
10. Homeyer, S. T., and Sachtler, W. M. H., *J. Catal.* **117,** 91 (1989).
11. Park, S. H., Tzou, M. S., and Sachtler W. M. H., *Appl. Catal.* **24,** 85 (1986).
12. Tzou, M. S. and Sachtler W. M. H., *in* "Catalysis" (J. W. Ward, Ed.) p. 233. Elsevier, 1987.
13. Sachtler W. M. H., Tzou, M. S., and Jiang, H. J., *Solid State Ionics* **26,** 71 (1988).
14. Chow, M., Park, S. H., and Sachtler W. M. H., *Appl. Catal.* **19,** 349 (1985).
15. Augustine, S. M., Alameddin, G. N., and Sachtler W. M. H., *J. Catal.* **115,** 217 (1989).
16. Lokhov, Yu., and Bredikhin, M., *Opt. Rep.* **1,** 12 (1990).
17. Homeyer, S. T., Karpiński, Z., and Sachtler W. M. H., *Recl. Trav. Chim. Pays-Bas* **109,** 81 (1990).
18. Lieske, H., Lietz, G., Spindler, H., and Völter, J., *J. Catal* **81,** (1983).
19. Chow, M., Park, S. H., and Sachtler W. M. H., *Appl. Catal.* **19,** 349 (1985).
20. Luck, F. Schmitt, J. L., and Marie G., *React. Kinet. Catal. Lett.* **21,** 219 (1982).
21. Jiang, H. J., Tzou, M. S., and Sachtler W. M. H., *Appl. Catal.* **39,** 255 (1988).
22. Moretti, G., and Sachtler W. M. H., *J. Catal.* **116,** 350 (1989).
23. Alvarez, W. E., and Resasco, D. E., *Catal. Lett.* **8,** 53 (1991).
24. Kustov, L. M., Ostgard, D., and Sachtler, W. M. H., *Catal. Lett.* **9,** 121 (1991).
25. Besoukhanova, C., Guidot, J., Barthomeuf, D., Breysse, D., and Bernard, J. R., *J. Chem. Soc. Faraday Trans.* **77,** 1595 (1981).
26. Larsen, G., and Haller G. L., *in* "Catalytic Science and Technology" p. 135. Kodansha, Tokyo, 1991.